Ternary Thallides *RE*MgTl (*RE* = Y, La – Nd, Sm, Gd – Tm, Lu)

Rainer Kraft and Rainer Pöttgen

Institut für Anorganische und Analytische Chemie, Westfälische Wilhelms-Universität Münster, Corrensstraße 36, D-48149 Münster, Germany

Reprint requests to R. Pöttgen. E-mail: pottgen@uni-muenster.de

Z. Naturforsch. **60b,** 265 – 270 (2005); received October 4, 2004

The rare earth metal (*RE*)–magnesium–thallides *RE*MgTl (*RE* = Y, La–Nd, Sm, Gd–Tm, Lu) were prepared from the elements in sealed tantalum tubes in a water-cooled sample chamber of a high-frequency furnace. The thallides were characterized through their X-ray powder patterns. They crystallize with the hexagonal ZrNiAl type structure, space group *P*62*m*, with three formula units per cell. Four structures were refined from X-ray single crystal diffractometer data: $a = 750.5(1)$, $c = 459.85(8)$ pm, $wR2 = 0.0491$, 364 F^2 values, 14 variables for YMgTl; $a = 781.3(1)$, $c = 477.84(8)$ pm, $wR2 = 0.0640$, BASF = 0.09(2), 425 F^2 values, 15 variables for LaMgTl; $a = 774.1(1)$, $c = 473.75(7)$ pm, $wR2 = 0.0405$, 295 F^2 values, 14 variables for CeMgTl; $a = 760.3(1)$, $c = 465.93(8)$ pm, $wR2 = 0.0262$, 287 F^2 values, 14 variables for SmMgTl. The PrMgTl, NdMgTl, GdMgTl, TbMgTl, and DyMgTl structures have been analyzed using the Rietveld technique. The *RE*MgTl structures contain two cystallographically independent thallium sites, both with tri-capped trigonal prismatic coordination: $Tl1Mg_3RE_6$ and $Tl2Mg_6RE_3$. Together the magnesium and thallium atoms form three-dimensional [MgTl] networks with Mg–Mg distances of 327 and Mg–Tl distances in the range 299 – 303 pm (data for CeMgTl).

Key words: Rare Earth Compounds, Thallides, Crystal Chemistry

Introduction

In continuation of our investigations on equiatomic *RETX* (*RE* = rare earth element; *T* = late transition element; *X* = main group element) intermetallics [1 – 3, and ref. therein], we have recently substituted the transition metal sites by magnesium in order to study the influence on the crystal chemistry and the physical properties. The transition metal–magnesium substitution strongly influences the hybridization of the rare earth element. It is therefore interesting to study the magnetic properties of the magnesium-based systems in parallel to those with the transition metals.

The series of gallides *RE*MgGa and indides *RE*MgIn have been synthesized and structurally characterized [4 – 7]. They crystallize with the hexagonal ZrNiAl type structure [8 – 10]. First magnetic characterizations revealed antiferromagnetic ordering at 3.1 K for CeMgGa [5] and at 22(2), 12(1), and 3(1) K for DyMgIn, HoMgIn, and TmMgIn, respectively [7]. Interestingly, isotypic GdMgIn shows no magnetic order down to 4 K [4].

Recent phase analytical investigations in the systems with the higher homologue thallium revealed the series of isotypic compounds *RE*MgTl (*RE* = Y, La–Nd, Sm, Gd–Tm, Lu). The synthesis and structural characterization of these compounds is reported herein.

Table 1. Lattice parameters of the hexagonal thallides *RE*MgTl (space group *P*62*m*, ZrNiAl type).

Compound	*a* [pm]	*c* [pm]	*V* [nm^3]
YMgTl	750.5(1)	459.85(8)	0.2243
LaMgTl	781.3(1)	477.84(8)	0.2526
CeMgTl	774.1(1)	473.75(7)	0.2458
PrMgTl	770.2(1)	471.50(7)	0.2422
NdMgTl	766.6(1)	469.45(5)	0.2389
SmMgTl	760.3(1)	465.93(8)	0.2333
GdMgTl	755.6(1)	463.12(7)	0.2290
TbMgTl	751.8(1)	460.88(8)	0.2256
DyMgTl	749.5(1)	459.32(8)	0.2235
HoMgTl	747.1(2)	458.35(8)	0.2215
ErMgTl	744.9(1)	457.15(6)	0.2197
TmMgTl	743.2(1)	455.41(6)	0.2178
LuMgTl	740.2(1)	454.00(6)	0.2154

Experimental Section

Synthesis

The ternary thallides were synthesized by using rare earth ingots (Johnson Matthey, Chempur or Kelpin, $> 99.9\%$), a

Table 2. Crystal data and structure refinement for *RE*MgTl (*RE* = Y, La, Ce, Sm; space group $P\bar{6}2m$; $Z = 3$).

Empirical formula	YMgTl	LaMgTl	CeMgTl	SmMgTl
Molar mass [g/mol]	317.59	367.59	368.80	379.03
Unit cell dimensions	Table 1	Table 1	Table 1	Table 1
Calculated density [g/cm^3]	7.05	7.25	7.47	8.10
Crystal size [μm^3]	$40\times60\times200$	$80\times120\times200$	$20\times60\times100$	$30\times30\times80$
Transm. ratio (max/min)	0.992 / 0.205	0.135 / 0.020	0.922 / 0.483	0.907 / 0.522
Absorption coefficient [mm^{-1}]	73.0	60.2	62.7	70.3
$F(000)$	396	450	453	465
θ Range [°]	3 to 35	3 to 35	3 to 30	3 to 30
Range in *hkl*	±12; ±12; $0 \le l \le 6$	±12; ±12; $-7 \le l \le 6$	±10; ±10; $-6 \le l \le 0$	±10; ±10; $-6 \le l \le 5$
Total no. reflections	1936	3531	1572	2611
Independent reflections	364 ($R_{int} = 0.0970$)	425 ($R_{int} = 0.1569$)	295 ($R_{int} = 0.0453$)	287 ($R_{int} = 0.0717$)
Reflections with $I > 2\sigma(I)$	344 ($R_{sigma} = 0.0489$)	412 ($R_{sigma} = 0.0612$)	289 ($R_{sigma} = 0.0234$)	281 ($R_{sigma} = 0.0316$)
Data/parameters	364 / 14	425 / 15	295 / 14	287 / 14
Goodness-of-fit on F^2	1.133	1.195	1.213	1.038
Final *R* indices [$I > 2\sigma(I)$]	$R1 = 0.0259$	$R1 = 0.0293$	$R1 = 0.0172$	$R1 = 0.0130$
	$wR2 = 0.0485$	$wR2 = 0.0631$	$wR2 = 0.0401$	$wR2 = 0.0261$
R Indices (all data)	$R1 = 0.0283$	$R1 = 0.0311$	$R1 = 0.0180$	$R1 = 0.0136$
	$wR2 = 0.0491$	$wR2 = 0.0640$	$wR2 = 0.0405$	$wR2 = 0.0262$
Extinction coefficient	0.036(2)	0.0067(5)	0.0124(7)	0.0207(9)
Flack parameter	0.05(5)	–	$-0.03(1)$	$-0.03(1)$
BASF	–	0.09(2)	–	–
Largest diff. peak and hole [e/Å^3]	2.82 and -1.66	2.12 and -2.51	1.42 and -1.86	1.07 and -1.09

Table 3. Atomic coordinates and isotropic displacement parameters (pm^2 for U_{eq} and Å^2 for B) for *RE*MgTl (space group $P\bar{6}2m$). U_{eq} is defined as a third of the trace of the orthogonalized U_{ij} tensor.

Atom	Wyckoff site	*x*	*y*	*z*	U_{eq}/B
YMgTl (single crystal data)					
Y	3*f*	0.5712(2)	0	0	75(2)
Mg	3*g*	0.2442(6)	0	1/2	89(8)
Tl1	2*d*	1/3	2/3	1/2	65(1)
Tl2	1*a*	0	0	0	87(2)
LaMgTl (single crystal data)					
La	3*f*	0.4237(1)	0	0	129(2)
Mg	3*g*	0.7552(8)	0	1/2	136(10)
Tl1	2*d*	2/3	1/3	1/2	134(2)
Tl2	1*a*	0	0	0	150(2)
CeMgTl (single crystal data)					
Ce	3*f*	0.4243(1)	0	0	94(2)
Mg	3*g*	0.7561(6)	0	1/2	91(9)
Tl1	2*d*	2/3	1/3	1/2	95(2)
Tl2	1*a*	0	0	0	107(2)
PrMgTl (powder data)					
Pr	3*f*	0.5751(2)	0	0	1.49(4)
Mg	3*g*	0.244(1)	0	1/2	1.0(2)
Tl1	2*d*	1/3	2/3	1/2	1.18(3)
Tl2	1*a*	0	0	0	1.55(6)
NdMgTl (powder data)					
Nd	3*f*	0.5747(2)	0	0	1.62(5)
Mg	3*g*	0.242(2)	0	1/2	1.5(3)
Tl1	2*d*	1/3	2/3	1/2	1.46(5)
Tl2	1*a*	0	0	0	1.86(7)

magnesium rod (Johnson Matthey, ∅ 16 mm, > 99.5%) and thallium granules (∅ 1 – 5 mm, Chempur > 99.999%, kept under water). All rare earth pieces with the notable excep-

Table 3 (continued).

Atom	Wyckoff site	*x*	*y*	*z*	U_{eq}/B
SmMgTl (single crystal data)					
Sm	3*f*	0.57295(7)	0	0	78(1)
Mg	3*g*	0.2437(4)	0	1/2	83(7)
Tl1	2*d*	1/3	2/3	1/2	73(1)
Tl2	1*a*	0	0	0	89(1)
GdMgTl (powder data)					
Gd	3*f*	0.5716(2)	0	0	1.28(5)
Mg	3*g*	0.243(1)	0	1/2	0.8(2)
Tl1	2*d*	1/3	2/3	1/2	1.25(4)
Tl2	1*a*	0	0	0	1.45(6)
TbMgTl (powder data)					
Tb	3*f*	0.5711(4)	0	0	1.4(1)
Mg	3*g*	0.244(2)	0	1/2	0.3(4)
Tl1	2*d*	1/3	2/3	1/2	0.70(7)
Tl2	1*a*	0	0	0	0.9(1)
DyMgTl (powder data)					
Dy	3*f*	0.5713(2)	0	0	1.36(4)
Mg	3*g*	0.241(1)	0	1/2	1.6(2)
Tl1	2*d*	1/3	2/3	1/2	1.01(3)
Tl2	1*a*	0	0	0	1.28(5)

Table 4. Interatomic distances (pm), calculated from single crystal data using the lattice parameters taken from X-ray powder data of CeMgTl.

Ce:	1 Tl2	328.5(1)	Mg:	2 Tl1	298.7(3)
	4 Tl1	330.9(1)		2 Tl2	302.9(3)
	2 Mg	349.4(3)		2 Mg	327.0(8)
	4 Mg	371.0(1)		2 Ce	349.4(3)
	4 Ce	400.1(1)		4 Ce	371.0(1)
Tl1:	3 Mg	298.7(3)	Tl2:	6 Mg	302.9(3)
	6 Ce	330.9(1)		3 Ce	328.5(1)

Table 5. X-ray powder data and structure refinement for PrMgTl, NdMgTl, GdMgTl, TbMgTl and DyMgTl (hexagonal, $P62m$, $Z = 3$).

Empirical formula	PrMgTl	NdMgTl	GdMgTl	TbMgTl	DyMgTl
Formula weight [g/mol]	369.60	372.93	385.94	387.62	391.19
Lattice parameters [pm]	$a = 771.43(2)$	$a = 768.16(1)$	$a = 756.624(8)$	$a = 753.05(1)$	$a = 750.006(8)$
(diffractometer data)	$c = 471.38(1)$	$c = 469.84(1)$	$c = 463.624(5)$	$c = 461.537(9)$	$c = 459.928(6)$
Cell volume [nm^3]	$V = 0.2429$	$V = 0.2401$	$V = 0.2299$	$V = 0.2267$	$V = 0.2241$
Calculated density [g/cm^3]	7.60	7.74	8.36	8.52	8.69
Absorption correction [μR]	1.40	1.40	1.40	1.40	1.40
$F(000)$	456	459	471	474	477
Range in 2θ	5 – 100	5 – 100	5 – 100	5 – 100	5 – 100
Scan mode, step width	$\theta/2\theta$, 0.03	$\theta/2\theta$, 0.03	$\theta/2\theta$, 0.03	$\theta/2\theta$, 0.03	$\theta/2\theta$, 0.03
No. data points	4751	4751	4751	4751	4751
Total no. Bragg reflections	79	79	76	75	75
Asymmetry parameters	0.03(2)	0.01(2)	0.03(1)	0.03(1)	0.03(1)
	0.020(3)	0.018(2)	0.018(2)	0.018(2)	0.024(2)
No. structure parameters	8	8	8	8	8
No. total parameters	16	16	16	16	16
R_F, R_{wp}	0.047, 0.094	0.066, 0.115	0.034, 0.085	0.055, 0.172	0.036, 0.081
$R_{Bragg(I)}$	0.048	0.058	0.045	0.072	0.049
(χ^2)	3.76	2.95	2.31	1.46	2.97
Bérar-Lelann Factor	3.92	2.84	2.72	1.74	2.82

tion of thulium (too high vapour pressure) were then melted to small buttons in an arc-melting apparatus [11] under purified argon. The argon (Westfalen, 4.8) was purified using heated titanium sponge (900 K), molecular sieve and silica gel. The magnesium pieces were cut from slices cut from said rod of which the outer edges were discarded in order to minimize surface impurities. The thallium granules were dried using paper towels, since for security reasons they were kept under water and then taken without further preparations. All such prepared starting materials were then weighed in the ideal 1:1:1 atomic ratios and put inside tantalum ampoules, which were subsequently sealed under purified argon (see above) of 800 mbar in a similar arc-welding apparatus. The prepared ampoule was then put inside a water-cooled quartz chamber [12] which in turn was inside the induction coil of a high-frequency generator (Hüttinger Elektronik Freiburg, Typ TIG 1.5/300).

The preparation involves two steps. The first one leads to a homogenous melt. The ampoule was put under flowing argon and a power output of approximately 65% led to the estimated temperature of about $\sim$ 1500 K. This state was kept for 10 min before reducing the power and the temperature to 28% ($\sim$ 950 K). This state was kept for another 4 h and then the power was cut thereby quenching the sample. The ampoule was in the inert argon atmosphere during the whole time. Excess reaction heat of the elements was visible during the first preparation step due to small flashs which spontaneously lighted up the tantalum ampoule. After the reaction container had attained room temperature it was removed, the sample was then broken from the walls with carefully executed hammer strokes and finally the ampoule was cut open using a tube cutter. The samples were extracted from the container as a mixture of small polycrystalline pieces which exhibited metallic lustre and powder which appeared black. Although the samples seem to be quite stable in air the metallic lustre turns to a dull black within a matter of weeks.

X-ray film data and single crystal structure refinement

All samples were analyzed through Guinier powder patterns using Cu-K$_{\alpha 1}$ radiation and α-quartz ($a = 491.30$, $c = 540.46$ pm) as an internal standard. The Guinier camera was equipped with an imaging plate system (Fujifilm BAS-1800). The lattice parameters (Table 1) were obtained from least-squares fits. To ensure correct indexing, the observed patterns were compared to calculated ones [13] using the atomic positions obtained from the structure refinements. The lattice parameters derived for the powders and the single crystals agreed well.

Irregularly shaped single crystals of YMgTl, LaMgTl, CeMgTl, and SmMgTl were isolated from the annealed samples by careful mechanical fragmentation. The crystals were subsequently examined by Laue photographs on a Buerger precession camera (equipped with an imaging plate system Fujifilm BAS-1800) in order to establish suitability for intensity data collection. Single crystal intensity data were collected at room temperature by use of a four-circle diffractometer (CAD4) with graphite monochromatized Mo-K$_\alpha$ (71.073 pm) radiation and a scintillation counter with pulse height discrimination. The scans were taken in the $\omega/2\theta$ mode and an empirical absorption correction was applied on the basis of psi-scan data, followed by a spherical absorption correction. All relevant crystallographic data for the data collections and evaluations are listed in Table 2.

The isotypy of these thallides with the previously reported gallium and indium compounds [4 – 7] was already evident from the X-ray powder data. The atomic positions of CeMgGa [5] were taken as starting values and the structures were refined using SHELXL-97 (full-matrix least-squares on F_o^2) [14] with anisotropic atomic displacement parameters for all sites.

As a check for the correct site assignment or possible Mg/Tl mixing, the occupancy parameters of all four crystals were refined in a separate series of least-squares cycles. All sites were fully occupied within two standard deviations. In the last cycles, the ideal occupancies were assumed again. Refinement of the correct absolute structure was ensured through refinement of the Flack parameter [15, 16]. In some cases, where the Flack parameter was close to 1, the atomic parameters were inverted and the structure was refined again. The LaMgTl crystal showed twinning by inversion with approximately 9% of the second domain, similar to SmMgGa and TmMgGa [6]. Final difference Fourier synthesis revealed no significant residual peaks (see Table 2). The positional parameters and interatomic distances are listed in Tables 3 and 4. Further details on the structure refinements are available.* The *RE*MgTl single crystal measured on the diffractometer have been analyzed by EDX using a LEICA 420 I scanning electron microscope. The semi-quantitative analyses (no standard was available for thallium) were close to the ideal compositions. No impurity elements were detected.

Rietveld data of PrMgTl, NdMgTl, GdMgTl, TbMgTl, and DyMgTl

High-quality single crystals were not obtained for all *RE*MgTl thallides. We have therefore investigated some of these compounds on a powder diffractometer (Stoe Stadi P, Cu-K$_{\alpha 1}$ radiation) in order to perform full profile Rietveld refinements. The data for PrMgTl, NdMgTl, and GdMgTl are presented in Fig. 1, those of TbMgTl and DyMgTl in Fig. 2. The measurements were performed in Debye-Scherrer geometry using Cu-K$_{\alpha 1}$ radiation ($\lambda = 154.0598$ pm, Ge monochromator). All experimental details are listed in Table 5.

The Rietveld calculations were performed with the FULLPROF [17] software. The background was set manually and the profiles were modelled using the pseudo-Voigt function. The limit of peak asymmetry was set to 60 degrees (2θ). The experimental data of the five refinements are summarized in Table 5. The standard deviations of the refined parameters have been multiplied with the Bérar-Lelann factor [18]. The refined positional parameters are listed in Table 3. The standard deviations of the *x* parameters for the rare earth metal and magnesium position are, as expected, significantly larger for the X-ray powder data as compared to the single crystal

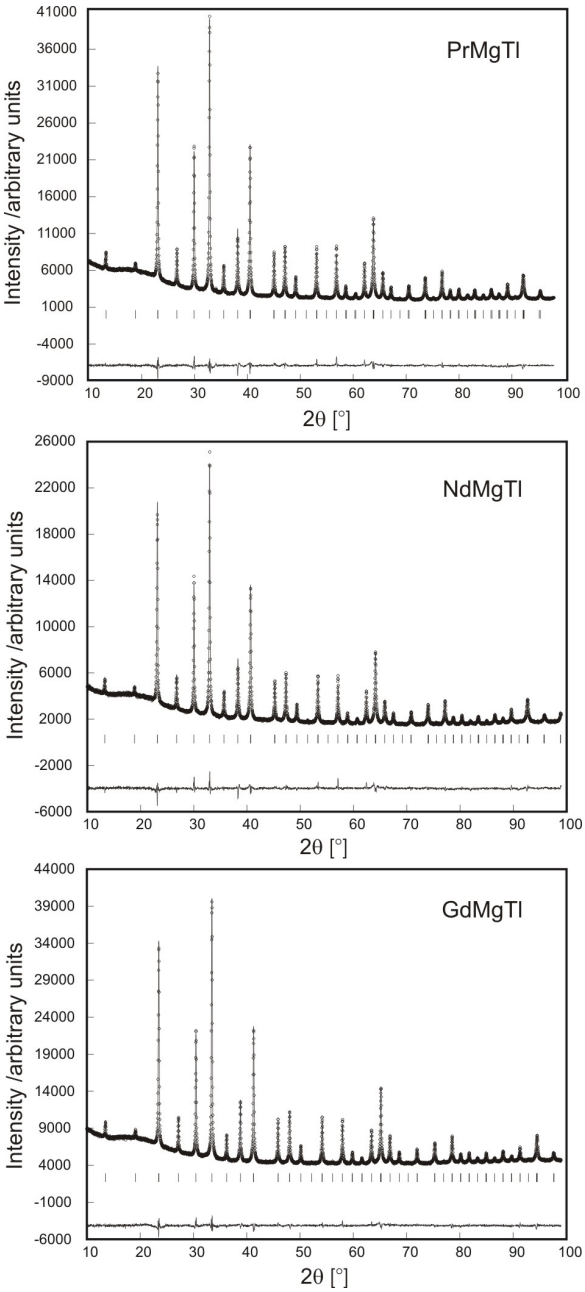

Fig. 1. Rietveld refinement plots for PrMgTl, NdMgTl, and GdMgTl, in which the observed intensites are indicated with open circles and the calculated pattern with a line on top of the circles. The vertical lines indicate the Bragg positions. The difference *y*(obs)-*y*(calc) is drawn below the Bragg indicators.

*Details may be obtained from: Fachinformationszentrum Karlsruhe, D-76344 Eggenstein-Leopoldshafen (Germany), by quoting the Registry No's. CSD 414438 (YMgTl), CSD 414439 (LaMgTl), CSD 414440 (CeMgTl), and CSD 414441 (SmMgTl).

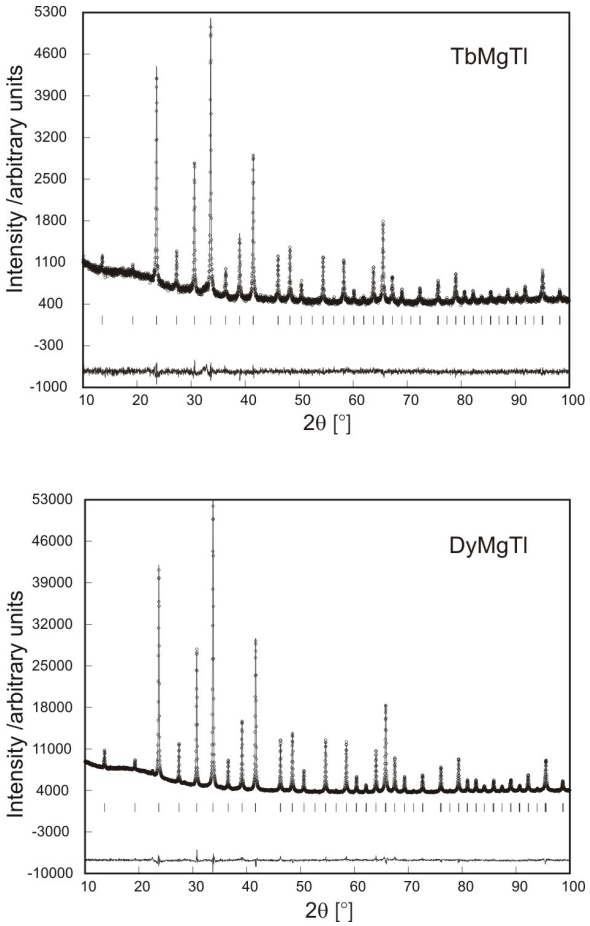

Fig. 2. Rietveld refinement plots for TbMgTl and DyMgTl, in which the observed intensites are indicated with open circles and the calculated pattern with a line on top of the circles. The vertical lines indicate the Bragg positions. The difference *y*(obs)-*y*(calc) is drawn below the Bragg indicators.

data. Nevertheless, the powder data fully confirm the structure of these compounds and we could show that these five samples are very pure on the level of X-ray powder diffraction.

Discussion

The 13 *RE*MgTl thallides reported herein crystallize with the hexagonal ZrNiAl type structure [8–10], a ternary ordered variant of the well known Fe_2P type [19, 20]. As emphasized in Fig. 3, the cell volumes decrease more or less monotonically from the lanthanum to the lutetium compound as expected from the lanthanide contraction. The volume of CeMgTl fits well between the volumes of LaMgTl and PrMgTl, indicating purely trivalent cerium in CeMgTl. The cell

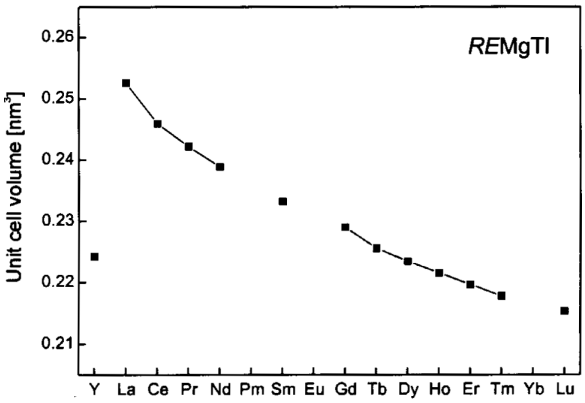

Fig. 3. Plot of the cell volumes of the hexagonal *RE*MgTl compounds.

volume of YMgTl fits between those of TbMgTl and DyMgTl, similar to the *RE*MgGa series [6], while YMgIn fits between DyMgIn and HoMgIn [7].

Binary Mg_2Tl [21] also crystallizes with the Fe_2P type ($a = 808.29(4)$, $c = 367.96(4)$ pm, $V = 0.2082$ nm^3). Formally, the *RE*MgTl thallides derive from Mg_2Tl by an ordered substitution of one magnesium site by the rare earth metal atoms. This substitution has a drastic effect on the lattice parameters. In the ternary thallides the *a* parameters are smaller by 30–70 pm, while the *c* parameters expand by up to 110 pm, leading to much higher c/a ratios for *RE*MgTl. Nevertheless, the rare earth metals have larger metallic radii than magnesium. Thus, the cell volumes of the ternary compounds are larger than that of Mg_2Tl. The drastic change in the c/a ratio is a direct consequence of the size of the rare earth metals. The *RE* atoms dominate the *c* parameter. Consequently the *a* parameters need to collapse in order to retain approximately the coordination at the atomic sites.

The crystal chemistry of the ZrNiAl related compounds has intensively been discussed in the literature [5, 9, 20, and ref. therein]. For more structural details and drawings of this simple structure we refer to previous work [5]. As an example we shortly discuss the interatomic distances in CeMgTl (Table 4). Within the three-dimensional [MgTl] network the Mg–Tl distances range from 299 to 303 pm, slightly longer than the sum of the covalent radii of 291 pm [22]. In binary Mg_2Tl the Mg–Tl distances cover the much broader range from 273 to 331 pm (calculated with the atomic positions of Mg_2In [23]). Some of the Mg–In interactions in Mg_2Tl are stronger than in the ternary thal-

lides. In MgTl [24] with CsCl structure, the Mg–Tl distance is 314 pm. The shortest Mg–Mg distance of 327 pm in CeMgTl is only slightly longer than the average Mg–Mg distance of 320 pm in *hcp* magnesium [25]. The short Mg–Mg distance in CeMgTl corresponds to the triangular faces of the trigonal prisms around Tl2. This is different in binary Mg_2Tl, where the edges of the triangles are at 350 pm Mg–Mg, while the Mg–Mg distances between these prisms are shorter.

With europium we obtained the new thallide EuMgTl. In contrast to the compounds listed here, EuMgTl contains divalent europium (7.9(1) μ_B/Eu atom in the paramagnetic state) and crystallizes with the orthorhombic TiNiSi type structure (*Pnma*, $a = 806.6(2)$, $b = 493.65(8)$, $c = 874.0(1)$ pm). The crystallographic data, the physical properties and an evaluation of chemical bonding will be reported elsewhere [26].

Acknowledgements

We thank B. Heying and Dipl.-Ing. U. Ch. Rodewald for the collection of the single crystal data, H.-J. Göcke for the work at the scanning electron microscope, and Dr. M. Valldor for helpful discussions concerning the Rietveld refinements. This work was financially supported by the Deutsche Forschungsgemeinschaft.

[1] R. Pöttgen, D. Johrendt, Chem. Mater. **12**, 875 (2000).
[2] R. Pöttgen, D. Johrendt, D. Kußmann, Structure Property Relations of Ternary Equiatomic YbTX Intermetallics, in K. A. Gschneidner (Jr.), L. Eyring (eds): Handbook on the Chemistry and Physics of Rare Earths, Vol. 32, chapter 207, Elsevier, Amsterdam (2001).
[3] R.-D. Hoffmann, R. Pöttgen, Z. Kristallogr. **216**, 127 (2001).
[4] F. Canepa, M. L. Fornasini, F. Merlo, M. Napoletano, M. Pani, J. Alloys Compd. **312**, 12 (2000).
[5] R. Kraft, D. Kaczorowski, R. Pöttgen, Chem. Mater. **15**, 2998 (2003).
[6] R. Kraft, M. Valldor, R. Pöttgen, Z. Naturforsch. **58b**, 827 (2003).
[7] R. Kraft, M. Valldor, D. Kurowski, R.-D. Hoffmann, R. Pöttgen, Z. Naturforsch. **59b**, 513 (2004).
[8] M. F. Zumdick, R.-D. Hoffmann, R. Pöttgen, Z. Naturforsch. **54b**, 45 (1999).
[9] A. E. Dwight, M. H. Mueller, R. A. Conner (Jr.), J. W. Downey, H. Knott, Trans. Met. Soc. AIME **242**, 2075 (1968).
[10] P. I. Krypyakevich, V. Ya. Markiv, E. V. Melnyk, Dopov. Akad. Nauk. Ukr. RSR, Ser. A, 750 (1967).
[11] R. Pöttgen, Th. Gulden, A. Simon, GIT Labor Fachzeitschrift **43**, 133 (1999).
[12] D. Kußmann, R.-D. Hoffmann, R. Pöttgen, Z. Anorg. Allg. Chem. **624**, 1727 (1998).
[13] K. Yvon, W. Jeitschko, E. Parthé, J. Appl. Crystallogr. **10**, 73 (1977).
[14] G. M. Sheldrick, SHELXL-97, Program for Crystal Structure Refinement, University of Göttingen, Germany (1997).
[15] H. D. Flack, G. Bernadinelli, Acta Crystallogr. A **55**, 908 (1999).
[16] H. D. Flack, G. Bernadinelli, J. Appl. Crystallogr. **33**, 1143 (2000).
[17] T. Roisnel, J. Rodríguez–Carvajal, Fullprof.2k V. 2.0 (2001) Laboratoire Léon Brillouin (CEA-CNRS), 91191 Gif-sur-Yvette Cedex (France).
[18] J.-F. Bérar, P. Lelann, J. Appl. Crystallogr. **24**, 1 (1991).
[19] S. Rundqvist, F. Jellinek, Acta Chem. Scand. **13**, 425 (1959).
[20] M. F. Zumdick, R. Pöttgen, Z. Kristallogr. **214**, 90 (1999).
[21] F. Frank, K. Schubert, J. Less-Common Met. **20**, 215 (1970).
[22] J. Emsley, The Elements, Oxford University Press, Oxford (1999).
[23] K. Schubert, F. Gauzzi, K. Frank, Z. Metallkd. **54**, 422 (1963).
[24] E. Zintl, G. Brauer, Z. Phys. Chem. **20B**, 245 (1933).
[25] J. Donohue, The Structures of the Elements, Wiley, New York (1974).
[26] R. Kraft, Yu. Grin, R. Pöttgen, unpublished results.